^{7}Li$(n, \gamma)^8$Li reaction and the S_{17} factor at $E_{\text{c.m.}} > 500$ keV

Y. Nagai,[1] M. Igashira,[2] T. Takaoka,[3,*] T. Kikuchi,[3,†] T. Shima,[1] A. Tomyo,[1,‡] A. Mengoni,[4,5,6] and T. Otsuka[4,6]
[1]*Research Center for Nuclear Physics, Osaka University, Ibaraki, Osaka 667-0047, Japan*
[2]*Research Laboratory for Nuclear Reactors, Tokyo Institute of Technology, O-okayama, Meguro, Tokyo 152-8550, Japan*
[3]*Department of Applied Physics, Tokyo Institute of Technology, O-okayama, Meguro, Tokyo 152-8551, Japan*
[4]*The Institute of Physical and Chemical Research (RIKEN), Wako, Saitama 351-01, Japan*
[5]*National Institute for New Technologies, Energy and Environment (ENEA), v. Don Fiammellei 2, I- 40128 Bologna, Italy*
[6]*Department of Physics, The University of Tokyo, Bunkyo, Tokyo 113-0033, Japan*
(Received 19 December 2004; published 19 May 2005)

The partial cross sections from the neutron capture state to the ground and first excited states in ^{8}Li have been separately determined for the first time at stellar neutron energy. The direct and weak cascade γ rays from the capture and first excited states to the ground state were measured by means of anti-Compton NaI(Tl) and anti-Compton HPGe spectrometers, respectively. The γ-ray branching ratio and the cross sections thus determined agree with that for thermal neutrons assuming a $1/v$ neutron velocity dependence. By comparing the cross sections with calculations based on the nonresonant direct capture mechanism it is shown that the cross sections are sensitive to the interaction potential of the incident neutron with the ^{7}Li target nucleus. This analysis confirms the possibility of deriving the parameters necessary for the calculation of the astrophysical S factor $S_{17}(E)$ for the ^{7}Be$(p, \gamma)^8$B reaction in the upper energy range above 500 keV.

DOI: 10.1103/PhysRevC.71.055803 PACS number(s): 25.40.Lw, 21.10.Jx, 26.65.+t, 29.30.Kv

I. INTRODUCTION

Of all the reactions relevant to the solar neutrino production, the cross section of the ^{7}Be$(p, \gamma)^8$B reaction is one of the reactions with the largest uncertainty [1]. The uncertainty is mainly a consequence of the fact that ^{7}Be is radioactive, and the cross section is very small and very difficult to measure. Hence, in order to accurately measure the cross section various approaches such as a direct (p, γ) reaction [2], the inverse Coulomb dissociation (CD) reaction [3], and/or heavy ion transfer reactions [4] have been employed. However, since the cross section at the Gamow energy of $kT \approx 20$ keV is too low to be measured experimentally using current techniques, the measured data taken at higher energies need to be extrapolated to low energy to determine the astrophysical $S_{17}(E)$ factor using theoretical calculations. Naturally, it is important that the various approaches used to derive $S_{17}(E = 0)$ produce consistent results, and theory should explain this consistent set of measurements. Recently, a detailed measurement of the ^{7}Be$(p, \gamma)^8$B reaction cross section has been carried out over the wide energy regions of between $E_{\text{c.m.}} = 116$ and 260 keV [5]. Through the comparison of the results with the values obtained using other reactions, it has been claimed that the energy dependence of the $S_{17}(E)$ factor differs significantly from the CD measurement over the wide energy range between 200 and 1400 keV. This discrepancy makes a meaningful comparison of the $S_{17}(0)$ factor quite difficult. Hence, in this latest direct measurement [5] the authors have only used their own experimental result to determine the $S_{17}(0)$. The extrapolation to low energies has been done using the theoretical calculation based on a cluster model [6] in which the normalization is chosen so as to fit the measured data at low energy. However, although the cluster model calculation together with fitted the 1^+ and 3^+ resonance states provides a reasonable value of the data up to 2500 keV, the agreement is not as good as it should be, in the higher energy regions of above 500 keV [5]. Hence, it is highly desirable to obtain the proper energy dependence of the $S_{17}(E)$ factor in order to determine $S_{17}(0)$ accurately and to clarify the origin of the different energy dependence of the $S_{17}(E)$ factor in the direct measurement and the CD measurement mentioned above.

Under such experimental and theoretical situations of the ^{7}Be$(p, \gamma)^8$B cross section, it is worthwhile to consider the use of another approach, such as the ^{7}Li$(n, \gamma)^8$Li reaction, for obtaining insights on the ^{7}Be$(p, \gamma)^8$B reaction cross section in the upper energy range [7]. The idea is to use the ^{7}Li$(n, \gamma)^8$Li cross section to constrain the key parameters required to obtain the ^{7}Be$(p, \gamma)^8$B cross section. In fact, the excitation function of the (n, γ) reaction of a nucleus can provide important information on the neutron-nucleus interaction in the continuum. A well known example is a $1/v$ law for an s-wave capture. In addition, the γ-ray branching ratio for transitions from a neutron capture state to low-lying states is also sensitive to the neutron interaction in the capture reaction process. So far, the partial cross section from the capture state to the ground state of ^{8}Li has been measured by several groups [8–13]. With reference to the discussion developed above we have concluded that it is necessary to measure the direct capture cross section to the ground and to the first excited states in ^{8}Li at higher neutron energies (see a partial level

*Present address: Nikon Corporation, 201-9, Miizugahara, Kumagaya Saitama, 360-8559, Japan.
†Present address: Hitachi, Ltd. 1-1, Saiwai-cho 3-chome, Hitachi-shi Ibaraki-ken, 317-8511, Japan.
‡Present address: Nissin Electric Co., Ltd., 47 Umezu-Takase-cho, Ukyo-ku, Kyoto 615-8686, Japan.

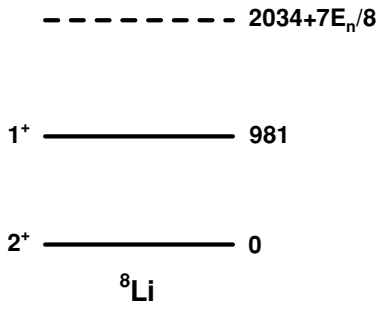

FIG. 1. Level scheme of ^{8}Li.

scheme of ^{8}Li in Fig. 1). Hence, in this study we aimed at determining the partial capture cross sections to the ground and first excited states in the keV region, from 10 to 80 keV.

II. EXPERIMENTAL PROCEDURE

The experiment was carried out by using a pulsed neutron beam and detecting prompt γ rays emitted in the ^{7}Li$(n, \gamma)^8$Li reaction. The partial capture cross sections to the ground ($\sigma_{\gamma 0}$) and to the first excited states ($\sigma_{\gamma 1}$) of ^{8}Li were determined by measuring the γ rays emitted in transitions leading to the ground state from the capture state and from the first excited states using high efficiency NaI(Tl) [14] and high resolution HPGe [15] spectrometers, respectively. The pulsed neutrons were produced by the ^{7}Li$(p, n)^7$Be reaction using a pulsed proton beam with a width of 1.5 ns, provided by the 3.2 MV Pelletron Accelerator of the Research Laboratory for Nuclear Reactors at the Tokyo Institute of Technology. An average beam current of 5 μA (10 μA) was obtained at a repetition rate of 2 MHz (4 MHz). The proton energy was adjusted so as to produce neutrons between 10 and 80 keV. The neutron energy spectrum was measured by a ^{6}Li-glass scintillation detector set at 8.7° with respect to the proton beam direction with a time-of-flight (TOF) method as shown in Fig. 2. The correction of the detector efficiency is made using an empirically determined

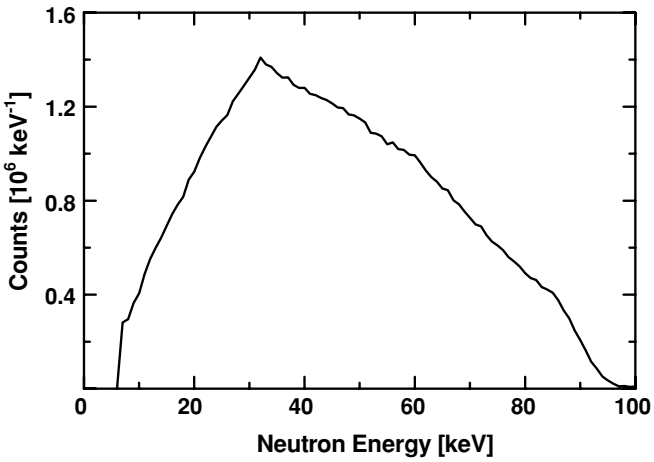

FIG. 2. Neutron energy spectrum measured by a ^{6}Li-glass scintillation detector with a TOF method. The energy dependent neutron detector efficiency was corrected for.

efficiency curve. A $^7Li_2O$ (99.94% enriched in ^{7}Li) was used as a sample, while a gold sample was used for normalization of the absolute capture cross section, since its cross section is known with good accuracy (within an uncertainty of 3–5%) [16]. The sample was placed at either 15 cm (in the measurement with the use of the NaI(Tl) spectrometer) or 12 cm (HPGe spectrometer) downward from the neutron target with respect to the proton beam direction. Special care was paid for preparing the hydrogen-free $^7Li_2O$ sample. In fact, the incident neutrons would lose their energy drastically after colliding with the hydrogen if this would be contained in the sample. Since the neutron capture cross section of a nucleus increases with decreasing the neutron energy, the neutrons are likely to be captured by ^{7}Li. If this scattering effect would not be properly corrected for, we would get a wrong neutron capture cross section of ^{7}Li. Although we correct for the effect using a Monte Carlo code as described later, the correction factor due to neutron scattering effects would become large, and thus the cross section would be determined with a large uncertainty. The hydrogen-free $^7Li_2O$ sample was made as follows. The enriched ^{7}Li(OH)H_2O was heated on a furnace in vacuum at about 1600° C to make a $^7Li_2O$ powder. The powder, thus made, was put into a mold with a diameter of 63.7 mm and a thickness of 18.8 mm. After the powder was pressed by a special tool, it was sintered on a furnace in vacuum. The mass spectrum of the sample thus prepared was measured using a quadrupole mass spectrometer, and the amounts of hydrogen turned out to be less than 10^{-4} of the Li sample. Here the neutron transmission with the energy from 1 to 80 keV was calculated for such amounts of hydrogen sample with use of the neutron total cross section by proton [17], and the resultant transmission is higher than about 99.993%. Hence the neutron scattering effect by such amounts of hydrogen is sufficiently small and does not influence the neutron capture cross section of the ^{7}Li$(n, \gamma)^8$Li reaction.

The measurement of the ^{7}Li$(n, \gamma)^8$Li reaction cross section was carried out cyclically by changing the $^7Li_2O$, Au samples and a blank position to smear out any possible modifications of the measurement conditions such as the deterioration of the Li neutron production target and beam intensity loss. The event rates of these samples were connected to the neutron counts detected by the ^{6}Li-glass detector. Measurements were made to check the possibility of changes of the incident neutron energy using the ^{6}Li-glass detector. It turned out that changes were of less than 2 keV during the measurement.

The prompt γ ray due to the direct neutron capture into the ground state of ^{8}Li and the low energy cascade γ ray from the the first excited state of ^{8}Li to the ground state were detected by four anti-Compton NaI(Tl) spectrometers [14] and an anti-Compton Ge (HPGe) spectrometer [15], respectively. Each of the NaI(Tl) spectrometers comprised the central NaI(Tl) detector with a diameter of 228.6 mm and a length of 203.2 mm surrounded by the plastic scintillation detector with an outer diameter of 330.2 mm and a length of 279.4 mm. The distance between the sample and the central NaI(Tl) detector was 637 mm. The HPGe spectrometer consisted of the central 436 cc Ge detector with a diameter of 79 mm and a thickness of 89 mm, surrounded by an annular NaI(Tl)

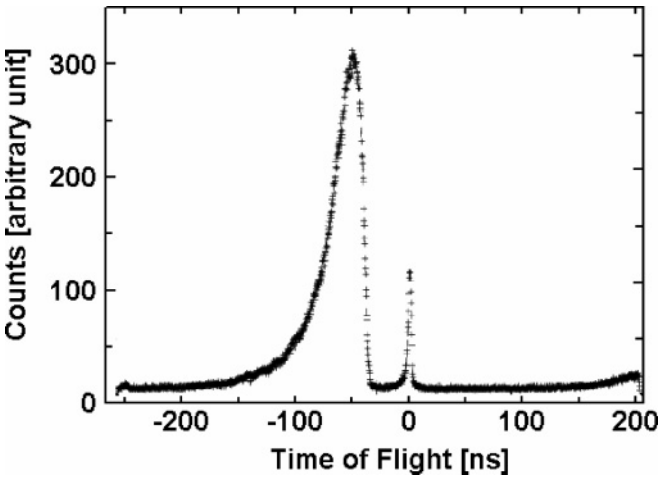

FIG. 3. Time-of-flight spectrum measured by the NaI(Tl) detector for the Au sample. The sharp peak at 0 ns is due to the γ ray from the ^{7}Li$(p, \gamma)^8$B reaction and the broad peak at -50 ns is due to the keV neutron capture by Au.

detector with an inner diameter of 112 mm, an outer diameter of 254 mm and a length of 305 mm. The distance between the sample and the HPGe detector was 746 mm. Note that it was hard to measure the weak low-energy cascade γ ray of about 1 MeV using the NaI(Tl) spectrometer, since the signal-to-noise (S/N) ratio of the spectrometer becomes worse at low energy region due to Compton tails from high energy γ rays. These spectrometers were set at 125.3° with respect to the proton beam direction, where the second Legendre polynomial is zero. Hence, the γ-ray intensity measured at this angle gives an angle-integrated γ-ray intensity for a dipole transition. Here, it should be mentioned that since both NaI(Tl) and Ge detectors are sensitive to neutrons, they were well shielded against neutron related background using ^{6}LiH, borated paraffin, lead, and Cd. All events taken by the NaI(Tl) spectrometers and the HPGe spectrometer were stored on a hard disk in an event mode.

III. RESULTS

A. γ-ray spectrum measured by NaI(Tl) spectrometers

The time-of-flight (TOF) spectrum measured for Au by the central NaI(Tl) detector is shown in Fig. 3. The sharp peak at 0 ns and the broad peak at around 50 ns are due to the ^{7}Li$(p, \gamma)^8$Be reaction at the neutron target position and due to the ^{197}Au$(n, \gamma)^{198}$Au reaction by keV neutrons, respectively. The foreground (FG: including a background component) and background (BG) γ-ray spectra for the ^{7}Li$(n, \gamma)^8$Li reaction are obtained by putting the gates on the proper regions on the TOF spectrum in Fig. 3, respectively. The TOF regions thus selected correspond to the neutron energy range from 10 to 30 keV, from 31 to 50 keV, and from 51 to 80 keV, respectively. The plateau region of between 30 and 100 ns on the TOF spectrum was selected to obtain the background γ-ray spectrum. Background subtracted γ-ray yields in these regions would provide us information on the energy dependence of the

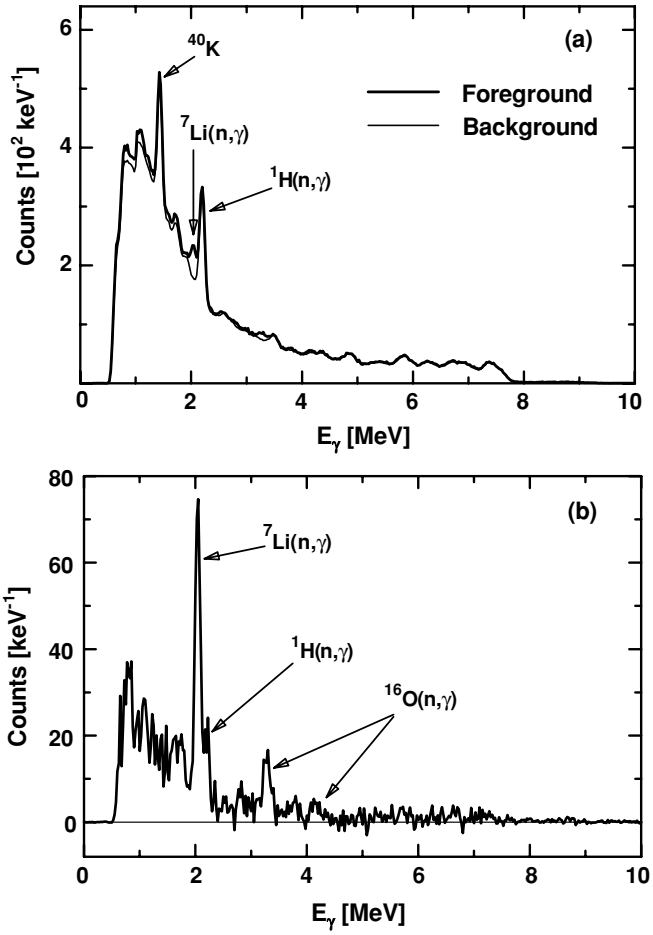

FIG. 4. γ-ray spectrum measured by an anti-Compton NaI(Tl) spectrometer. Foreground (solid line), background (dotted line) spectra (a), and a background subtracted spectrum (b). In the background subtracted spectrum the discrete γ rays of 2.07 MeV are due to the ^{7}Li$(n, \gamma)^8$Li reaction, of 2.25 MeV due to the $p(n, \gamma)D$ reaction, of 3.30 and 4.17 MeV are due to the ^{16}O$(n, \gamma)^{17}$O reaction, respectively.

cross section of the ^{7}Li$(n, \gamma)^8$Li reaction and on the neutron capture reaction mechanism as described later. The energy binning mentioned above was made so as to balance the statistics of the γ-ray yields of one energy region with that of another region. Typical FG and BG spectra are shown in Fig. 4(a), and a background subtracted (net) γ-ray spectrum is shown in Fig. 4(b) for the neutron energy of 31 $\sim$50 keV, respectively. In the net spectrum we can clearly see a discrete γ ray of 2070 $(2034 + 7E_n/8)$ keV due to the direct neutron capture into the ground state in ^{8}Li. The cascade γ rays with the 1092 $(1053 + 7E_n/8)$ keV and 981 keV peaks, which are the γ-ray transitions leading to the ground state via the 981 keV first excited state in ^{8}Li, and the 871 keV γ ray due to the deexcitation of the first excited state of ^{17}O populated by the ^{16}O$(n, \gamma)^{17}$O reaction to the ground state should be contained in the low energy region around 1 MeV in Fig. 4(b). Although there are structures, which may indicate these peaks, the peaks are not clear because their intensities are weak and there is a large Compton tail due to high energy γ rays. Note that the 2245 $(2224.5 + E_n/2)$ keV γ ray from the $p(n, \gamma)D$

reaction is also observed in the net spectrum because we used a thin polyethylene sheet to cover the $^7Li_2O$ sample. The 2070 keV γ-ray yield was obtained accurately by separating the contribution of the 2245 keV γ ray using the response function of the NaI(Tl) spectrometer as discussed below. Two discrete γ rays of 3300 and 4170 keV are due to the direct neutron capture of ^{16}O into the first excited and ground states of ^{17}O [18], respectively. The background γ rays in Fig. 4(a) are due to natural radio activities such as that of ^{40}K (at 1461 keV), ^{208}Tl (at 2615 keV), and γ rays from the $p(n,\gamma)D$ and the ^{56}Fe$(n,\gamma)^{57}$Fe reactions induced by neutrons thermalized by the collision of incident neutrons with various materials in the experimental room. Net γ-ray spectra for neutrons of $10 \sim 30$ keV and $51 \sim 80$ keV are obtained by the similar process mentioned above.

The intensity of the discrete γ-ray peak in Fig. 4(b) was analyzed using the response function of the spectrometer, which was obtained using the γ rays from the standard source such as ^{60}Co, ^{88}Y, and from the ^{19}F$(p,\alpha\gamma)^{16}$O and ^{27}Al$(p,\gamma)^{28}$Si reactions [14]. The partial capture cross section ($\sigma_{\gamma 0}$) for the γ ray for the ^{7}Li$(n,\gamma_0)^8$Li leading to the ^{8}Li ground state was obtained using the γ-ray intensity

$$\sigma_\gamma(\mathrm{Au}) = C\frac{(\phi)_{\mathrm{Au}}}{(\phi)_{\mathrm{Li}}}\cdot\frac{(r^2n)_{\mathrm{Au}}}{(r^2n)_{\mathrm{Li}}}\cdot\frac{Y_\gamma(\mathrm{Li})}{Y_\gamma(\mathrm{Au})}\cdot\sigma_\gamma(\mathrm{Au}). \quad (1)$$

Here, ϕ(Au) and Y_γ(Au) are the yields of the neutron and of the γ ray for Au, respectively, σ_γ(Au) is the absolute capture cross section of Au, r and n are the radius and thickness (atoms/barn) of the sample, respectively. A correction factor C, product of the four factors $C_{\mathrm{nm}}, C_{\mathrm{ns}}, C_{\gamma a}$, and $C_{\gamma g}$, is defined as

$$C = \frac{(C_{\mathrm{nm}}C_{\mathrm{ns}}C_{\gamma a}C_{\gamma g})_{\mathrm{Au}}}{(C_{\mathrm{nm}}C_{\mathrm{ns}}C_{\gamma a}C_{\gamma g})_{\mathrm{Li}}}\ . \quad (2)$$

Here the factor C_{nm} is introduced to correct for a multiple-scattering effect of the incident neutron in a sample; namely, it corrects for the overestimation of the γ-ray yield due to neutrons scattered in the sample. The factor C_{ns} is introduced to correct for the shielding of the incident neutrons in the sample, since the flux of the incident neutron is attenuated due to scattering and/or absorption in the sample. The factors of C_{nm} and C_{ns} were calculated using the Monte Carlo code, TIME-MULTI [19]. The $C_{\gamma a}$ and $C_{\gamma g}$ factors are for the γ-ray absorption by the sample, and the finite size of the sample, respectively, and were also calculated by a Monte Carlo method. The correction factors thus obtained for Li_2O and Au samples are listed in Table I, respectively.

The partial cross section, $\sigma_{\gamma 0}$, obtained at average neutron energies of 20.6, 37.8, and 58.1 keV resulted to be 44.4(37), 33.7(26), and 30.7(26) μbarns, respectively (see Table II). The quoted uncertainty is the result of the combined uncertainties on the statistics of the γ-ray yield, of the response function of the NaI(Tl) spectrometer, of the absolute cross section of Au, and of the extrapolation of the γ-ray yields of Au to the low-energy side.

TABLE I. Correction factors used in the analysis for ^{7}Li and ^{197}Au at the averaged neutron energies of 20.6, 37.8, and 58.1 keV, respectively.

Averaged neutron energy	^{7}Li			^{197}Au		
E_n(keV)	C_{nm}	C_{ns}	$C_{\mathrm{nm}}\times C_{\mathrm{ns}}$	C_{nm}	C_{ns}	$C_{\mathrm{nm}}\times C_{\mathrm{ns}}$
20.6	1.62	0.83	1.35	1.24	0.93	1.16
37.8	1.37	0.84	1.15	1.20	0.94	1.13
58.1	1.25	0.85	1.05	1.17	0.94	1.11

B. γ-ray spectrum measured by the Ge spectrometer

The TOF spectrum measured for ^{7}Li by the HPGe spectrometer is shown in Fig. 5. The small peak at 0 ns and the broad one at around -40 ns are due to the ^{7}Li$(p,\gamma)^8$Be reaction and due to the keV neutron capture reaction by ^{7}Li, respectively. Here, the yield of the former peak is smaller than that for the NaI(Tl) spectrometer shown in Fig. 3 because a thicker lead shield was placed at the neutron target position to protect the HPGe detector from the radiation damage. The foreground spectrum was obtained by putting the gate in the wide neutron energy region of $20 \sim 70$ keV in the TOF spectrum to obtain a sufficient yield for the weak cascade γ rays. The background one was obtained by putting the gate in the plateau region of between 360 and 450 channels in the TOF spectrum. The foreground, background and net spectra are shown in Figs. 6(a)–6(b), and 6(c), respectively. In Fig. 6(c) we observed for the first time the 981 keV γ ray due to the deexcitation of the first excited state of ^{8}Li to the ground state at stellar neutron energy, and the broad 2073 $(2034 + 7E_n/8)$ keV γ ray due to the direct neutron capture into the ground state. The background γ rays were due to neutrons scattered by the ^{7}Li sample and various materials in the experimental room. Here the 981 keV γ ray was assigned to be due to the ^{7}Li$(n,\gamma)^8$Li reaction by referring its energy and studying background spectrum as discussed below. The energy calibration of the HPGe detector was made using standard γ-ray sources such as ^{60}Co, ^{88}Y, and ^{137}Cs, and natural activities of ^{40}K (at 1461 keV) and ^{208}Tl (at 2615 keV). In the analysis of the background spectrum in Fig. 6(b) we also used the spectrum taken without the neutron beam, from which γ rays from the decays of ^{40}K (at 1461 keV), ^{228}Ac (at 795, 911, 965, and 969 keV), ^{212}Bi (at 727 keV), ^{214}Bi (at 609, 768, 786, 806, 1120, 1238, 1378, 1730, 1765, 1847, 2119, 2204, 2448 keV), and ^{206}Tl (at 583, 2615 keV) were identified in addition to

TABLE II. Measured and calculated cross sections (μb) at the averaged neutron energies of 20.6, 37.8, and 58.1 keV, respectively.

	Experiment		DRC calculation	
E_n(keV)	σ(g.s.) [μb]	σ(total) [μb]	σ(g.s.) [μb]	σ(total) [μb]
20.6	44.4 ± 3.7	49.8 ± 4.3	43.0	47.4
37.8	33.7 ± 2.6	37.8 ± 3.0	32.6	36.0
58.1	30.7 ± 2.6	34.5 ± 3.1	25.7	28.4

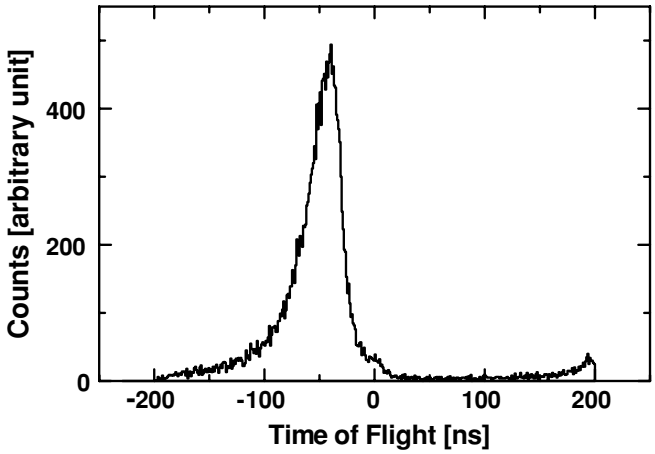

FIG. 5. Time-of-flight spectrum measured by the HPGe detector for the Au sample. The small peak at 0 ns is due to the γ ray from the ^{7}Li$(p, \gamma)^8$B reaction and the broad peak at -40 ns is due to the keV neutron capture by Au.

the 478 keV γ ray from the ^{7}Be produced by the^{7}Li$(p, n)^7$Be reaction at the neutron target position. The background γ rays caused by the neutrons were assigned to be due to the neutron capture reaction by ^{35}Cl (at 1951 keV), ^{56}Fe (at 1613 keV and 1725 keV), ^{70}Ge (at 708 keV, 1096 keV, 1778 keV, and 1941 keV), and ^{73}Ge (at 596 keV, 608 keV, and 1941 keV), respectively. The origin of most γ rays except weak ones observed in Figs. 6(a)–(c), was thus identified. Here, it would be worthwhile to discuss the correctness of the background subtraction we made in the present analysis. It can be found by comparing the observed shape of the γ-ray spectrum from the $p(n, \gamma)D$ reaction in the foreground spectrum to that in the net spectrum. In the foreground spectrum we observed two γ-ray peaks from the reaction with a narrow width at 2225 keV and a broad one at 2247 $(2224.5 + E_n/2)$ keV. The latter peak is due to the keV neutron capture reaction by hydrogen in the polyethylene film, which was used to cover the Li sample. The former one is due to the capture reaction induced by thermalized neutrons by hydrogen not only in the polyethylene film but also in other materials such as the B-doped paraffin and/or the ^{6}LiH. In the net spectrum, we only see the broad peak as shown in Fig. 6(c), which means that the background γ ray caused by thermalized neutrons is correctly subtracted. The broad 1092 $(1053 + 7E_n/8)$ keV γ-ray peak due to the direct neutron capture into the first excited state of ^{8}Li could not be identified due to the broadening of the peak width and the weakness of the γ-ray intensity. The 871 keV γ ray in Fig. 6(c) is due to the γ transition from the deexcitation of the first excited state of ^{17}O populated by the ^{16}O$(n, \gamma)^{17}$O reaction to the ground state.

The intensities of the 981 and 2073 keV peaks were analyzed using the γ-ray efficiency curve of the Ge detector, which was obtained by using standard γ-ray sources such as ^{60}Co, ^{88}Y, and ^{137}Cs. The relative intensity was obtained as

$$\frac{I_\gamma(\text{c.s.} \rightarrow \text{g.s.})}{I_\gamma(\text{c.s.} \rightarrow \text{g.s.}) + I_\gamma(\text{c.s.} \rightarrow \text{1st})} = 0.89 \pm 0.01. \quad (3)$$

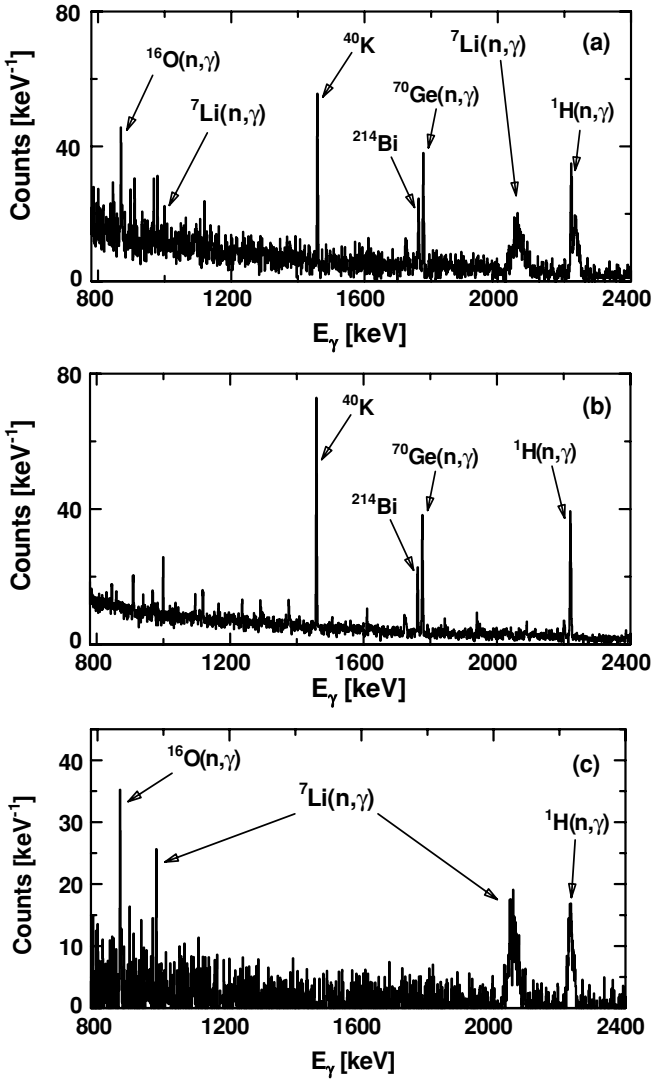

FIG. 6. γ-ray spectrum measured by an anti-Compton HPGe spectrometer for ^{7}Li. Foreground (a), background (b), and background subtracted spectra (c). In Fig. 4(c), the 981 keV γ ray from the first excited state in ^{8}Li to the ground state is clearly observed together with the 2073 keV γ ray from the neutron capture state of ^{7}Li to the ground state. The peak width of the latter peak is wide due to the neutron energy width of about 50 keV captured by ^{7}Li.

Here I_γ(c.s. $\rightarrow$ g.s.) and I_γ(c.s. $\rightarrow$ 1st) are the γ-ray intensities for the transitions leading to the ground and first excited states, respectively. The relative intensity obtained in the present study agrees with that for thermal neutrons, which indicates that the ^{7}Li$(n, \gamma)^8$Li reaction proceeds dominantly by an *s*-wave neutron capture process. With the use of the present result of the relative intensity together with the partial capture cross section of the direct neutron capture into the ground state of ^{8}Li the total cross section of the ^{7}Li$(n, \gamma)^8$Li reaction is derived as 49.9(42), 37.9 (29), and 34.5 (29) μb at average neutron energies of 20.6, 37.8, and 58.1 keV, respectively. The resultant cross sections agree with most of the previous data [8,10–13] as shown in Fig. 7 together with theoretical calculations based on a direct radiative capture

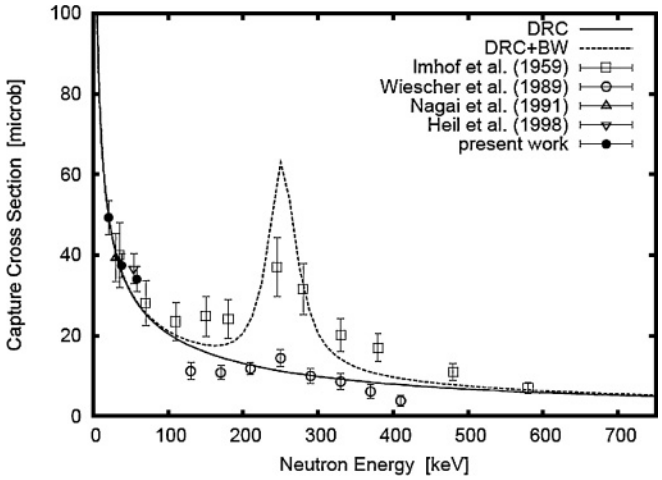

FIG. 7. The cross section of the ^{7}Li$(n,\gamma)^8$Li reaction obtained in the present study (black circle) and in the previous studies. The direct radiative capture calculations are shown as solid (DRC) and dotted (DRC+BW) lines.

process. The resultant partial capture cross sections to the first excited and ground states in ^{8}Li provide crucial information on the neutron nucleus interaction in the continuum, which is quite important to obtain the energy dependence of the $S_{17}(E)$ factor in the high energy region as discussed below.

IV. COMPARISON OF THE PRESENT EXPERIMENTAL RESULTS WITH A DIRECT CAPTURE MODEL

The neutron capture in ^{7}Li proceeds through direct radiative transitions to the ground ($J^\pi = 2^+$) and to the first excited ($J^\pi = 1^+$) states in ^{8}Li as shown in Fig. 1. In order to compare the present results with a theoretical value we have performed the calculations of the ^{7}Li$(n,\gamma)^8$Li cross section for energies covering the full range from thermal up to the MeV region within the framework of the direct radiative capture model (DRC), following the prescription of Ref. [20].

Within the DRC model, the matrix elements for electromagnetic transitions of electric L multipolarity $Q(\mathrm{EL})_{c\to b} = \langle \Psi_c || T^{\mathrm{EL}} || \Psi_b \rangle$ may be written as a product of three factors $Q(\mathrm{EL})_{c\to b} = \mathrm{I}_{c,b}\mathrm{B}_b\mathrm{A}_{c,b}$, where $\tau_{cb}^{\mathrm{EL}} = \int \psi_{EclcJc}(r) r^l \phi_{nblbjb}(r) dr$ is the overlap integral between the radial components of the continuum and bound state wave functions Ψ_c and Ψ_b, respectively, and $T^{\mathrm{EL}} = r^L Y_{\mathrm{LM}}$ is the electric multipole operator. The quantity B_b represents the fractional parentage coefficient for a single-particle configuration of the bound state (spectroscopic factor) and $A_{c,b}$ an angular momentum coupling coefficient. The quantum numbers defining the initial continuum state E_c, l_c, j_c, are coupled to form states with total angular momentum J_c, and similarly for the final bound state n_b, l_b, j_b are coupled to total angular momentum J_b.

The radial wave functions $\psi_{Eclcjc}(r)$ and $\phi_{nblbjb}(r)$ are obtained by solving the scattering and the bound state problem respectively, in a given potential. In the present case, a Woods-Saxon form of the potential has been adopted, with radius and diffuseness parameters $r_0 = 1.25$ fm and $d = 0.65$ fm, respectively. The potential well depth has been adjusted in order to reproduce the experimental scattering length $a_+ = -3.63 \pm 0.05$ fm and $a_- = +0.87 \pm 0.05$ fm for the two components, of the channel spin s at thermal energies. The resulting well depth parameters are $V_0 = 56.15$ MeV and $V_0 = 46.50$ MeV, for the $s = 2$ and $s = 1$ spin components, respectively.

The capture cross section is given by

$$\sigma_{c\to b}^{(\mathrm{EL})} = \frac{8\pi(L+1)}{L\,[(2L+1)!!]^2}\frac{k_\gamma^{2L+1}}{\hbar v}\frac{1}{(2s+1)}\frac{1}{(2I+1)} \times e_{\mathrm{EL}}^2 \sum_{lcjc,lbjb} \left|Q_{c\to b}^{(\mathrm{EL})}\right|^2, \quad (4)$$

where $k_\gamma = \varepsilon_\gamma/\eta c$ is the wave number for a transition emitting a γ ray with energy ε_γ, $e = -Z/A$ is the effective charge for neutrons.

The resulting neutron capture cross sections obtained in the present calculations are presented in Table II. The result for the thermal cross section, $\sigma(n_{\mathrm{th}},\gamma) = 46.0$ mb, is in very good agreement with the experimental value $\sigma^{\mathrm{exp}}(n_{\mathrm{th}},\gamma) = 45.4 \pm 3.0$ mb. This value has been obtained using the experimentally determined spectroscopic factors for the ground and first excited states in ^{8}Li: $S_{\mathrm{dp}}(\mathrm{g.s.}) = 0.87$ and $S_{\mathrm{dp}}(1\mathrm{st}) = 0.48$. The radial wave functions for the two bound states have been obtained using the same Woods-Saxon potential parameters as those used for the calculation of the continuum states, with the energy fixed to the experimental binding energies of $E_{\mathrm{gs}} = 2.033$ MeV and $E_{1\mathrm{st}} = 1.052$ MeV for the ground ($J^\pi = 2^+$) and first excited ($J^\pi = 1^+$) states, respectively.

The branching ratio $\mathrm{BR} = \sigma_{\gamma 0}/(\sigma_{\gamma 0} + \sigma_{\gamma 1})$ is equal to 0.91 at thermal energies, to be compared to the experimental value of Lynn *et al.* [20] of 0.89 ± 0.01. The DRC mechanism dominates the neutron capture process in the fast neutron energy region as well. This can be inferred from a comparison of the present experimental results on the branching ratio (BR) with the results of the DRC calculation. In fact, this value remains constant up to 100 keV as can be seen in Table II, as experimentally observed here. This result is particularly interesting for its implication in the evaluation of the astrophysical S factor for the ^{7}Be$(p,\gamma)^8$B reaction, S_{17}. In fact, while the very low energy limit of this quantity is mostly determined by the nuclear structure properties of the ^{8}B ground state, a suitable effective interaction potential for the p+^{7}Be interaction in the continuum is essential for the evaluation of the S_{17}, in particular in the energy range above, say, 500 keV. We have performed a set of calculations of the S_{17} using the same DRC model as the one just described for the representation of the ^{7}Li$(n,\gamma)^8$Li reaction. We are not concerned with the absolute value of this quantity here, but rather with its energy variation, in particular in the upper energy range. It should be stressed again that the energy dependence of the $S_{17}(E)$ differs significantly between the direct measurement and the CD measurement over the wide energy range between 200 and 1400 keV [5]. In the ^{7}Be$(p,\gamma)^8$B case, there is only one bound state, the ^{8}B$(J^\pi = 2+)$ ground state. Assuming a unity spectroscopic factor for this state, the resulting S_{17} is shown in Fig. 8. It is clear from the figure that, using a standard value of

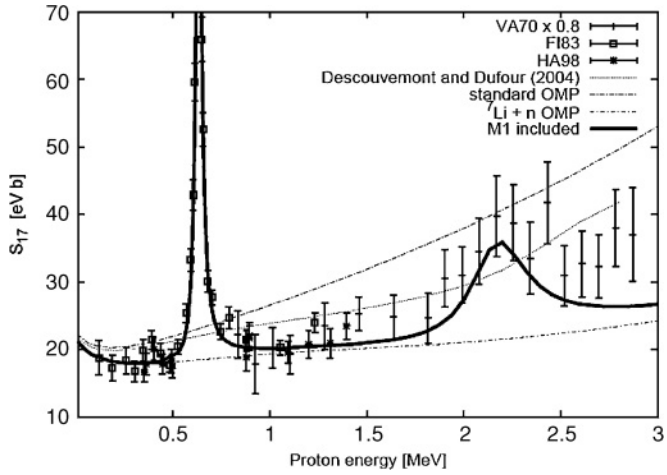

FIG. 8. Astrophysical S factor for the ^{7}Be$(p,\gamma)^8$B reaction in the proton energy range up to 3 MeV. The calculation performed with "standard OMP" refers to a DRC calculation with $V_0 = 50.0$ MeV. The other DRC calculation is performed using the effective potential derived from the ^{7}Li$(n,\gamma)^8$Li as described in the text. The $M1$ resonances at 723 and 2495 keV have been included with parameters ($\Gamma = 37$ and 350 keV), ($\Gamma_\gamma = 25$ and 150 meV, respectively).

the effective interaction potential for the continuum s- and d-scattering waves, one does not obtain a reliable description of the capture process in the upper energy side region. On the other hand, using the potential derived in the present study from the ^{7}Li$(n,\gamma)^8$Li reaction, a realistic description of the capture process is obtained in the full energy range up to 3 MeV. The recent calculation based on a microscopic cluster model [21] is shown for comparison in Fig. 8. While this calculation shows an improvement over the crude potential model, the result does not exhibit a satisfactory agreement with the experimental data in the high energy region, the main concern of the present work. From this analysis it can be therefore concluded that the use of a different interaction potential for the two different spin channels is essential in the representation of the particle-nucleus interaction (n-^{7}Li in the present case) in the continuum.

V. CONCLUSION

In the present study, we observed for the first time both γ rays due to the direct neutron capture into the ground and first excited states of ^{8}Li for $E_n = 10 \sim 80$ keV, respectively, and we determined their partial cross sections using these γ-ray yields. From the comparison of the measured cross sections with calculated ones based on a nonresonant direct capture mode, we could derive the effective interaction potential for the n+^{7}Li interaction in the continuum. Using the present result and assuming the charge symmetry of the nuclear interaction we could derive the energy dependence of the astrophysical S_{17} factor, which should be reliable in particular in the energy range above, say, 500 keV. Since the energy dependence of the $S_{17}(E)$ differs significantly between the direct measurement and the CD measurement over the wide energy range between 200 and 1400 keV, the present result could be quite important to clarify the origin of the discrepancy. It should be mentioned that high efficiency NaI(Tl) and high resolution HPGe spectrometers with good signal-to-noise ratio played essential roles in the detection of the weak γ rays.

ACKNOWLEDGMENTS

We thank T. Ohsaki, M. Kinoshita, T. Kobayashi, and F. Okazaki for their help in the experiments. This work was supported by a grant-in-aid for Specially Promoted Research of the Japan Ministry of Education, Science, Sports and Culture.

[1] E. G. Adelberger *et al.*, Rev. Mod. Phys. **70**, 1265 (1998).

[2] R. W. Kavanagh, Nucl. Phys. **15**, 411 (1960); P. D. Parker, Phys. Rev. **150**, 851 (1966); B. W. Filippone, A. J. Elwyn, C. N. Davids, and D. D. Koetke, Phys. Rev. C **28**, 2222 (1983); F. Hammache *et al.*, Phys. Rev. Lett. **86**, 3985 (2001); L. Gialanella *et al.*, Eur. Phys. J. A **7**, 30 (2000); M. Hass *et al.*, Phys. Lett. **B462**, 237 (1999); F. Strieder *et al.*, Nucl. Phys. **A696**, 219 (2001); A. R. Junghans, E. C. Mohrmann, K. A. Snover, T. D. Steiger, E. G. Adelberger, J. M. Casandjian, H. E. Swanson, L. Buchmann, S. H. Park, and A. Zyuzin, Phys. Rev. Lett. **88**, 041101 (2002); L. T. Baby *et al.*, Phys. Rev. C **67**, 065805 (2003).

[3] T. Motobayashi *et al.*, Phys. Rev. Lett. **73**, 2680 (1994); T. Kikuchi *et al.*, Eur. Phys. J. A **3**, 213 (1998); N. Iwasa *et al.*, Phys. Rev. Lett. **83**, 2910 (1999); B. Davids, *et al.*, *ibid.* **86**, 2750 (2001); F. Schumann *et al.*, *ibid.* **90**, 232501 (2003).

[4] A. Azhari, V. Burjan, F. Carstoiu, C. A. Gagliardi, V. Kroha, A. M. Mukhamedzhanov, F. M. Nunes, X. Tang, L. Trache, and R. E. Tribble, Phys. Rev. C **63**, 055803 (2001); L. Trache, F. Carstoiu, C. A. Gagliardi, and R. E. Tribble, Phys. Rev. Lett. **87**, 271102 (2001).

[5] A. R. Junghans *et al.*, Phys. Rev. C **68**, 065803 (2003).

[6] P. Descouvemont and D. Baye, Nucl. Phys. **A567**, 341 (1994).

[7] T. A. Tombrello, Nucl. Phys. **71**, 459 (1965); F. C. Barker and R. H. Spear, Astrophys. J. **307**, 847 (1988).

[8] W. L. Imhof *et al.*, Phys. Rev. **114**, 1037 (1959).

[9] M. Wiescher, R. Steininger, and F. Kaeppeler, Astrophys. J. **344**, 464 (1989).

[10] J. E. Lynn, E. T. Jurney, and S. Raman, Phys. Rev. C **44**, 764 (1991).

[11] Y. Nagai, M. Igashira, N. Mukai, T. Ohsaki, F. Uesawa, K. Takeda, T. Ando, H. Kitazawa, S. Kubono, and T. Fukuda, Astrophys. J. **381**, 444 (1991).

[12] M. Heil, F. Kaeppeler, M. Wiescher, and A. Mengoni, Astrophys. J. **507**, 997 (1998).

[13] J. C. Blackmon, A. E. Champagne, J. K. Dickens, J. A. Harvey, M. A. Hofstee, S. Kopecky, D. C. Larson, D. C. Powell, S. Raman, and M. S. Smith, Phys. Rev. C **54**, 383 (1996).

[14] T. Ohsaki, Y. Nagai, M. Igashira, T. Shima, T. S. Suzuki, T. Kikuchi, T. Kobayashi, T. Takaoka, M. Kinoshita, and Y. Nobuhara, Nucl. Instrum. Methods Phys. Res. A **425**, 302 (1999).

[15] M. Igashira, K. Tanaka, and K. Masuda, *Proceedings of the Conference of the 8th International Symposium on Capture Gamma-Ray and Related Topics* (World Scientific, Singapore, 1993), p. 992.

[16] ENDF/B-VI, data file for ^{197}Au (Mat = 7925), evaluated by S. F. Mughabghab.

[17] K. Shibata *et al*., J. Nucl. Sci. Technol. **39**, 1125 (2002).

[18] M. Igashira, Y. Nagai, K. Masuda, T. Ohsaki, and H. Kitazawa, Astrophys. J. Cett. **441**, L89 (1995).

[19] K. Senoo, Y. Nagai, T. Shima, T. Ohsaki, and M. Igashira, Nucl. Instrum. Methods Phys. Res. A **339**, 556 (1995).

[20] J. E. Lynn, E. T. Jurney, and S. Raman, Phys. Rev. C **44**, 764 (1991); A. Mengoni, T. Otsuka, and M. Ishihara, *ibid*. **52**, R2334 (1995).

[21] P. Descouvemont and M. Dufour, Nucl. Phys. **A738**, 150 (2004).